

SUPPORTING INFORMATION

Be₃B₁₁⁻ cluster: A dynamically fluxional beryllio-borospherene†

Ying-Jin Wang,^{*a} Lin-Yan Feng,^a Miao Yan,^a and Hua-Jin Zhai^{*b}

^a*Department of Chemistry, Xinzhou Teachers University, Xinzhou 034000, China*

^b*Nanocluster Laboratory, Institute of Molecular Science, Shanxi University, Taiyuan 030006, China*

*E-mail: yingjinwang@sxu.edu.cn; hj.zhai@sxu.edu.cn

Supplementary Information – Part I

- Table S1.** Cartesian coordinates for (a) the global-minimum (GM) (C_{2v} , 1A_1), (b) the local minimum (LM) (C_s , $^1A'$), and (c) the transition state (TS) (C_1 , 1A) structures of Be₃B₁₁⁻ cluster at the PBE0/6-311+G* level.
- Figure S1.** Alternative optimized structures of Be₃B₁₁⁻ cluster at the PBE0/6-311+G* level, the relative energies (in eV) are shown in square bracket with the corrections of zero-point energies (ZPEs), as well as for top four isomers at the single-point CCSD(T)/6-311+G*//PBE0/6-311+G* level.
- Figure S2.** The bond distances (in Å) obtained at the PBE0/6-311+G(d) level for (a) the GM (C_{2v} , 1A_1) and (b) the LM (C_s , $^1A'$) structures of Be₃B₁₁⁻ cluster.

- Figure S3.** Calculated Wiberg bond indices (WBIs) in black and natural atomic charges (in $|e|$) in blue for (a) the GM (C_{2v} , 1A_1) and (b) the LM (C_s , $^1A'$) of $\text{Be}_3\text{B}_{11}^-$ cluster from natural bond orbital (NBO) analyses at the PBE0/6-311+G* level.
- Figure S4.** The parameters of (a) bond distances, (b) Wiberg bond indices (WBIs) and (c) natural atomic charges in $|e|$ for TS (C_1 , 1A) structure of $\text{Be}_3\text{B}_{11}^-$ cluster. The WBIs and natural atomics are obtained from the natural bond orbital (NBO) analysis at the PBE0/6-311+G* level.
- Figure S5** Born-Oppenheimer molecular dynamic simulations for $\text{Be}_3\text{B}_{11}^-$ cluster at (a) 300 K, (b) 400 K, and (c) 600 K for 50 ps using the software suite CP2K. Some typical GM structures are picked up during the dynamic simulations. The root-mean-square-deviation (RMSD) and maximum bond length deviation (MAXD) values (on average) are indicated.
- Figure S6.** The canonical molecular orbitals (CMOs) for the GM (C_{2v} , 1A_1) of $\text{Be}_3\text{B}_{11}^-$ cluster. (a) Thirteen σ CMOs for ten Lewis two-center two-electron (2c-2e) B–B σ bonds in B_{11} skeleton, two three-center two-electron (3c-2e) and one six-center two-electron (6c-2e) delocalized σ bonds on two B_3 triangles. (b) Four radials π CMOs for three delocalized π bonds on waist and one delocalized π bond on two B_3 triangles. (c) Three tangential π CMOs for three delocalized π bonds on waist.
- Figure S7.** The CMOs for the LM (C_s , $^1A'$) of $\text{Be}_3\text{B}_{11}^-$ cluster. (a) Thirteen σ CMOs for eleven Lewis 2c-2e B–B σ bonds in B_{11} skeleton, one 3c-2e σ bond on bottom B_3 triangle and one 7c-2e delocalized σ bond on the top B_4 pyramid and bottom B_3 triangle. (b) Four radials π CMOs for three delocalized π bonds on waist and one delocalized π bond on top B_4 pyramid and bottom B_3 triangle. (c) Three tangential π CMOs for three delocalized π bonds on waist.
- Figure S8.** Electron localization functions (ELFs) for (a) the GM (C_{2v} , 1A_1), (b) the LM (C_s , $^1A'$) and (c) the TS (C_1 , 1A) structures.
- Figure S9.** The CMOs for the TS (C_1 , 1A) of $\text{Be}_3\text{B}_{11}^-$ cluster. (a) Thirteen σ CMOs for eleven 2c-2e B–B σ bonds in B_{11} skeleton, one 3c-2e σ bonds on bottom B_3 triangle and

one 7c-2e delocalized σ bond on top B_4 pyramid bottom B_3 triangle. (b) Four radials π CMOs for three delocalized π bonds on waist and one delocalized π bond on top B_4 pyramid and bottom B_3 triangle. (c) Three tangential π CMOs for three delocalized π bonds on waist.

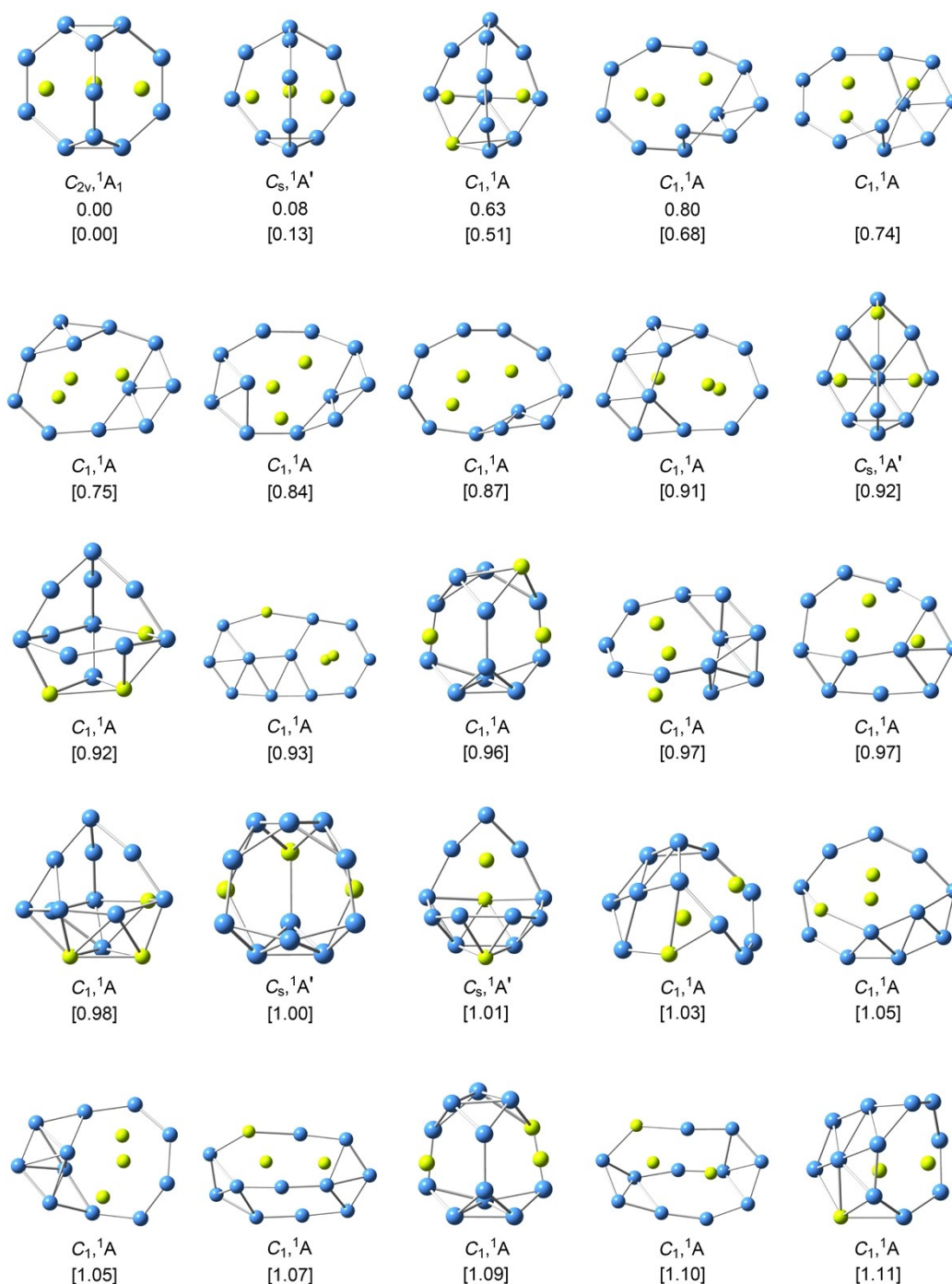
Figure S10. The adaptive natural density partitioning (AdNDP) bonding pattern for the TS (C_1 , 1A) structure of $Be_3B_{11}^-$ cluster. The occupation numbers (ONs) are indicated.

Figure S11. The evolution process of the delocalized (a) 6c-2e σ bond and (b) 6c-2e π bond on two B_3 triangles during the interconversion between the GM and LM.

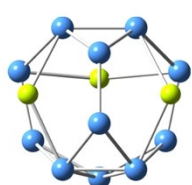
Supplementary Information – Part II

A **short movie** extracted from the BOMD simulation for $Be_3B_{11}^-$ cluster. The simulation was performed at the temperature of 600 K for 50 ps, starting from the equilibrium GM structure with random atom velocities. The movie roughly covers a time span of 12 ps.

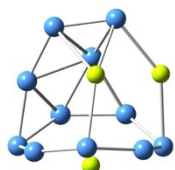
Figure S1. Alternative optimized structures of $\text{Be}_3\text{B}_{11}^-$ cluster at the PBE0/6-311+G* level, the relative energies (in eV) are shown in square bracket with the corrections of zero-point energies (ZPEs), as well as for top four isomers at the single-point CCSD(T)/6-311+G**/PBE0/6-311+G* level.



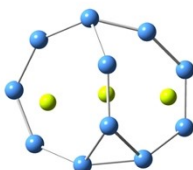
(continued ...)



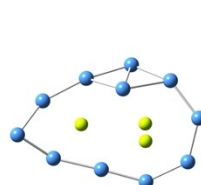
$C_s, ^1A'$
[1.12]



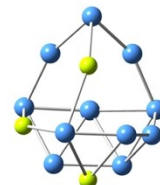
$C_1, ^1A$
[1.13]



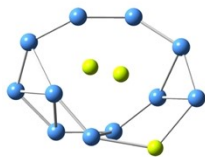
$C_1, ^1A$
[1.17]



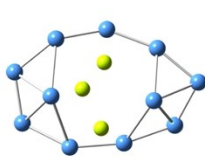
$C_1, ^1A$
[1.17]



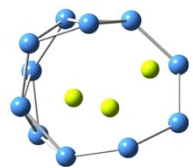
$C_1, ^1A$
[1.17]



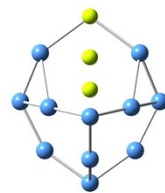
$C_1, ^1A$
[1.18]



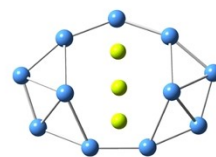
$C_1, ^1A$
[1.19]



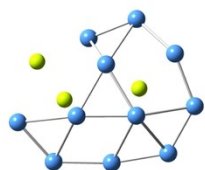
$C_1, ^1A$
[1.20]



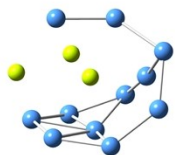
$C_s, ^1A'$
[1.21]



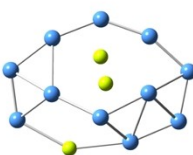
$C_s, ^1A'$
[1.22]



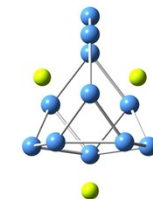
$C_1, ^1A$
[1.22]



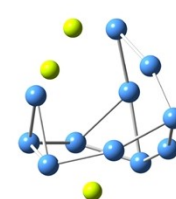
$C_1, ^1A$
[1.22]



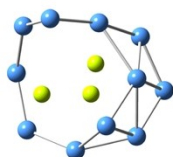
$C_1, ^1A$
[1.22]



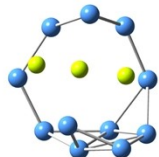
$C_s, ^1A'$
[1.23]



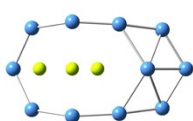
$C_1, ^1A$
[1.25]



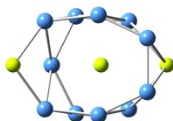
$C_1, ^1A$
[1.25]



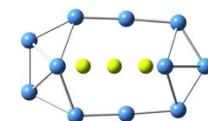
$C_1, ^1A$
[1.31]



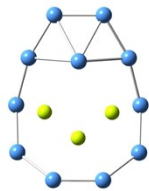
$C_1, ^1A$
[1.33]



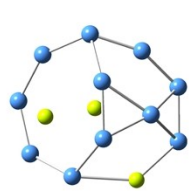
$C_s, ^1A'$
[1.37]



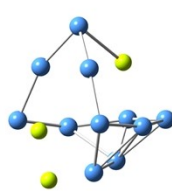
$C_s, ^1A'$
[1.37]



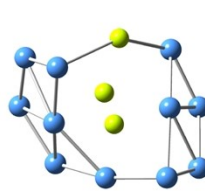
$C_s, ^1A'$
[1.40]



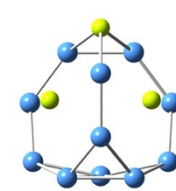
$C_1, ^1A$
[1.41]



$C_1, ^1A$
[1.41]

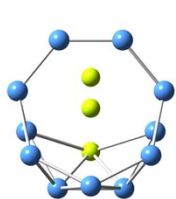


$C_1, ^1A$
[1.43]

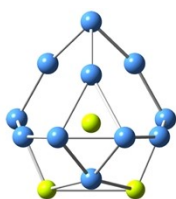


$C_s, ^1A'$
[1.44]

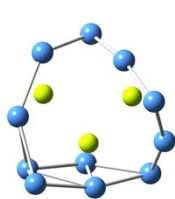
(continued ...)



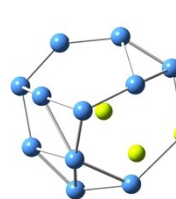
$C_s, 1A'$
[1.44]



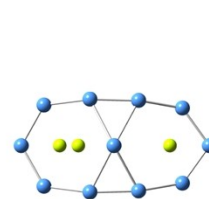
$C_s, 1A'$
[1.46]



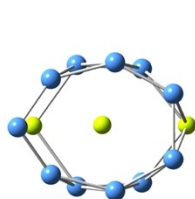
$C_1, 1A$
[1.48]



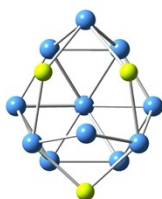
$C_1, 1A$
[1.49]



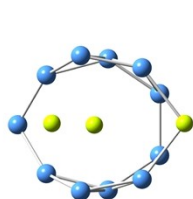
$C_s, 1A'$
[1.49]



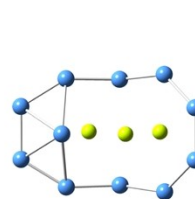
$C_s, 1A'$
[1.53]



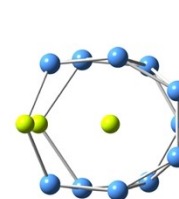
$C_s, 1A'$
[1.76]



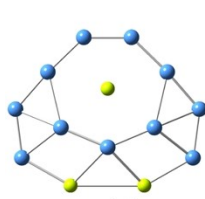
$C_s, 1A'$
[1.84]



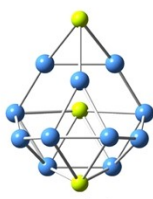
$C_s, 1A'$
[1.96]



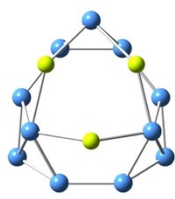
$C_s, 1A'$
[1.98]



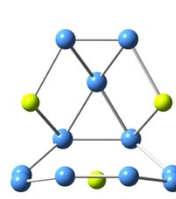
$C_s, 1A'$
[1.98]



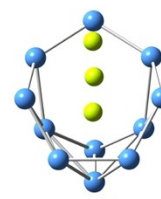
$C_s, 1A'$
[2.02]



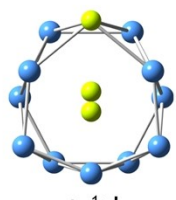
$C_s, 1A'$
[2.17]



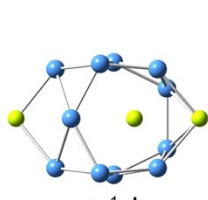
$C_s, 1A'$
[2.24]



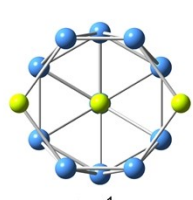
$C_s, 1A'$
[1.32]



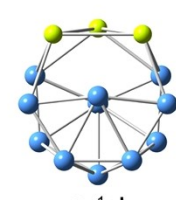
$C_s, 1A'$
[2.40]



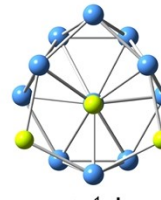
$C_s, 1A'$
[2.55]



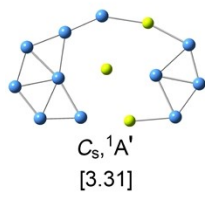
$C_{2v}, 1A_1$
[2.76]



$C_s, 1A'$
[2.82]



$C_s, 1A'$
[3.15]



$C_s, 1A'$
[3.31]

Figure S2. The bond distances (in Å) obtained at the PBE0/6-311+G(d) level for (a) the GM (C_{2v} , 1A_1) and (b) the LM (C_s , $^1A'$) structures of $Be_3B_{11}^-$ cluster.

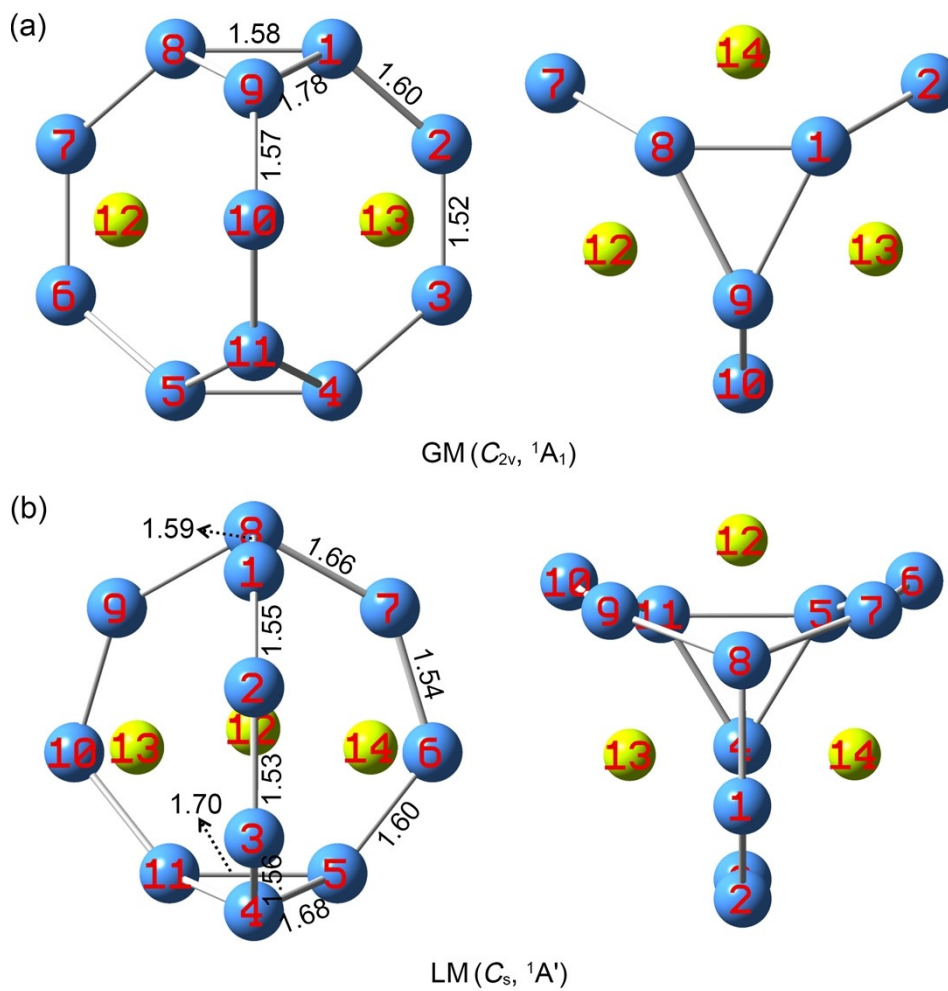


Figure S4. The parameters of (a) bond distances, (b) Wiberg bond indices (WBIs) and (c) natural atomic charges in $|e|$ for TS (C_1 , 1A) structure of $\text{Be}_3\text{B}_{11}^-$ cluster. The WBIs and natural atoms are obtained from the natural bond orbital (NBO) analysis at the PBE0/6-311+G* level.

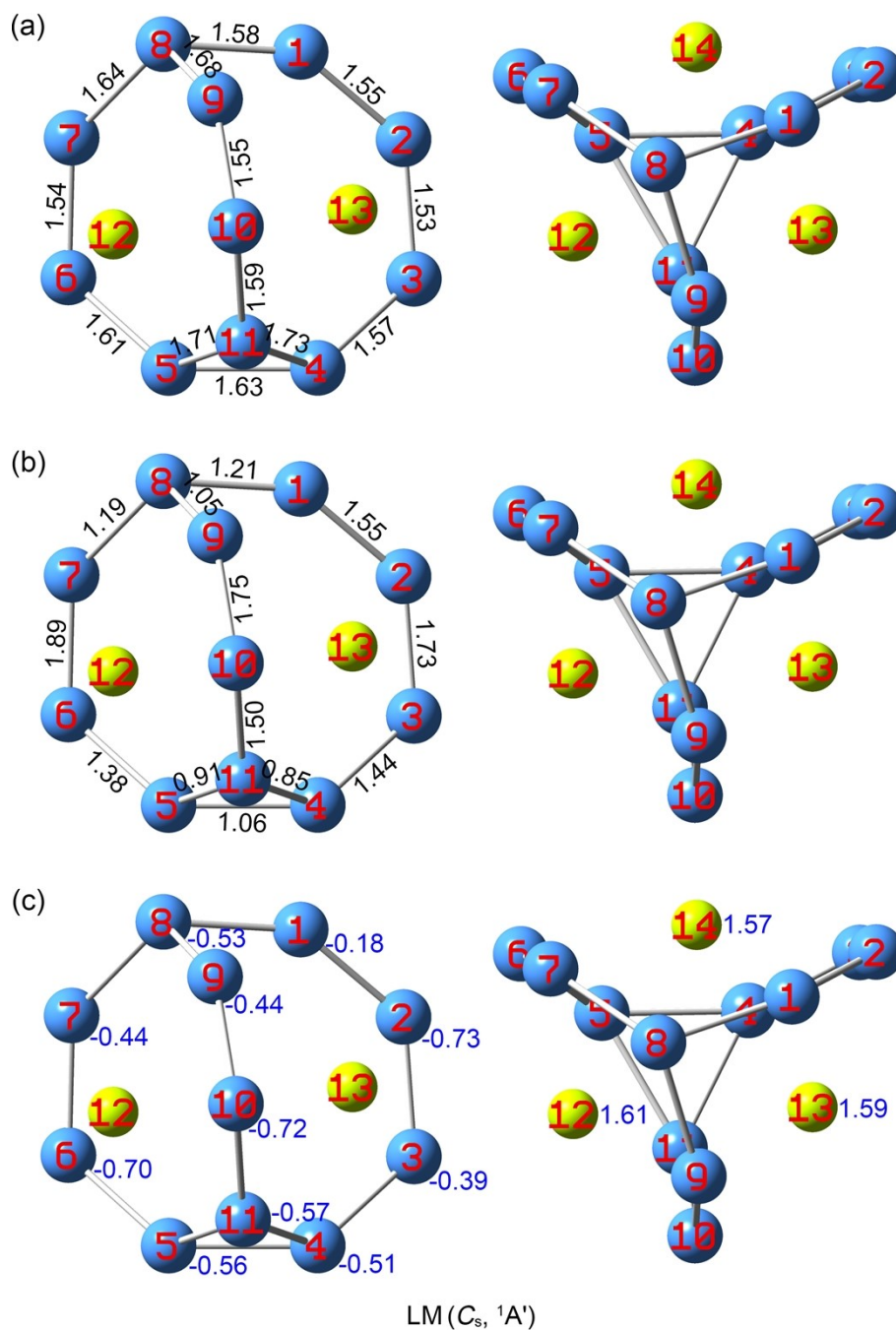


Figure S5 Born-Oppenheimer molecular dynamic simulations for $\text{Be}_3\text{B}_{11}^-$ cluster at (a) 300 K, (b) 400 K, and (c) 600 K for 50 ps using the software suite CP2K. Some typical GM structures are picked up during the dynamic simulations. The root-mean-square-deviation (RMSD) and maximum bond length deviation (MAXD) values (on average) are indicated.

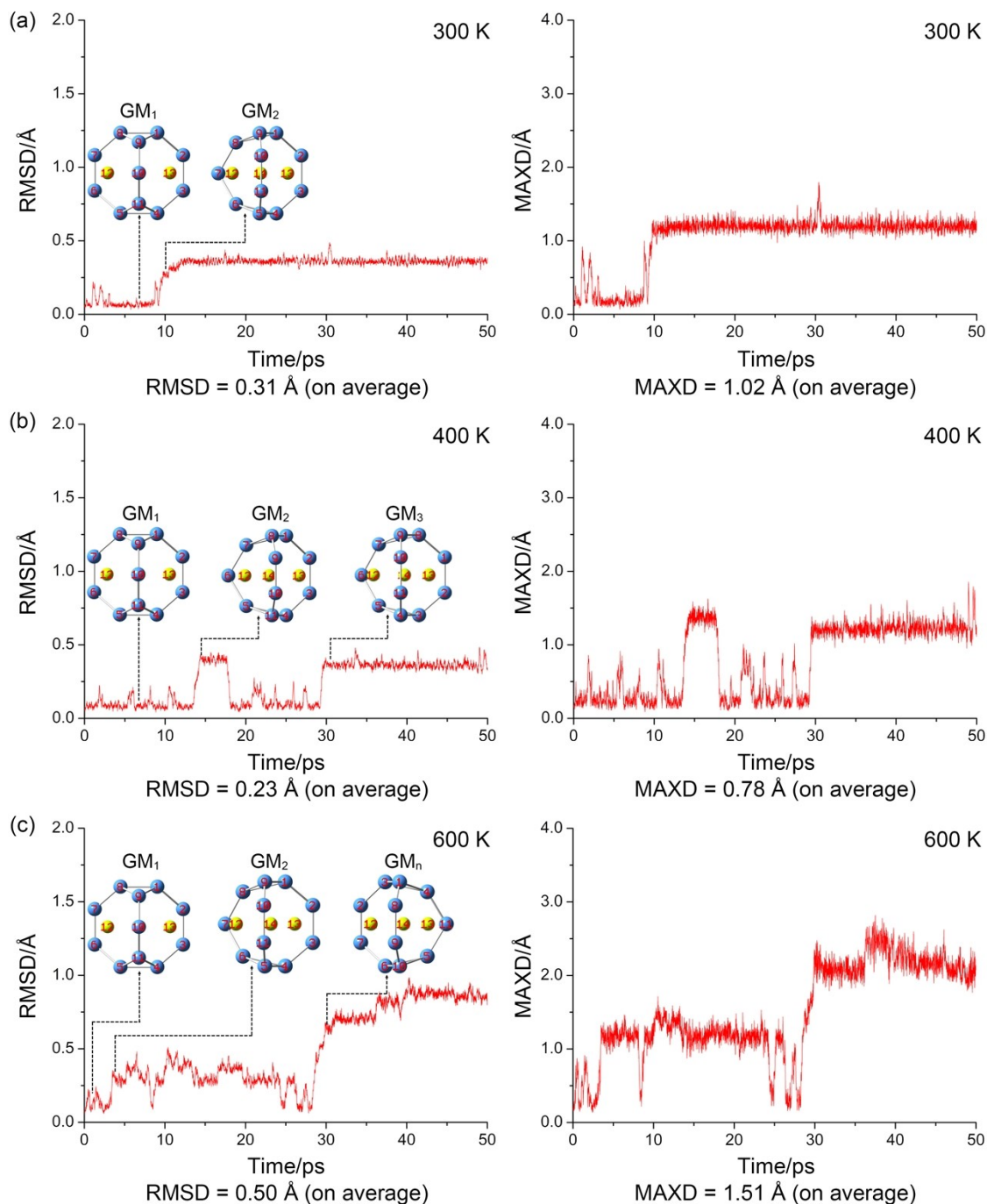


Figure S6. The canonical molecular orbitals (CMOs) for the GM (C_{2v} , 1A_1) of $\text{Be}_3\text{B}_{11}^-$ cluster. (a) Thirteen σ CMOs for ten Lewis two-center two-electron (2c-2e) B–B σ bonds in B_{11} skeleton, two three-center two-electron (3c-2e) and one six-center two-electron (6c-2e) delocalized σ bonds on two B_3 triangles. (b) Four radials π CMOs for three delocalized π bonds on waist and one delocalized π bond on two B_3 triangles. (c) Three tangential π CMOs for three delocalized π bonds on waist.

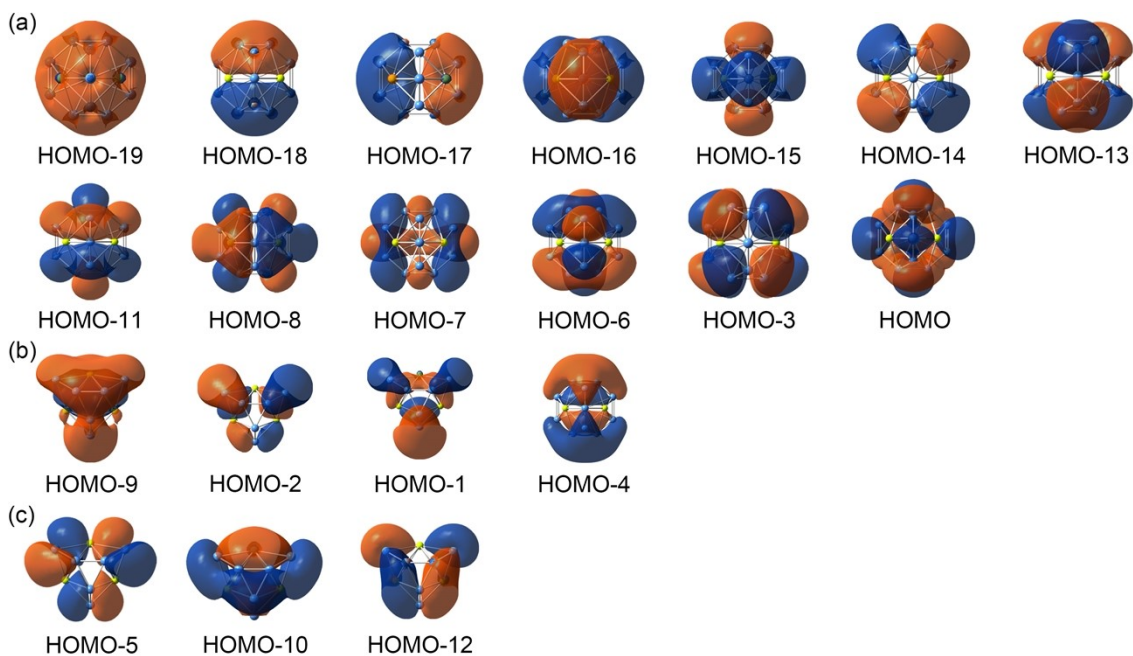


Figure S7. The CMOs for the LM (C_s , $^1A'$) of $Be_3B_{11}^-$ cluster. (a) Thirteen σ CMOs for eleven Lewis 2c-2e B–B σ bonds in B_{11} skeleton, one 3c-2e σ bond on bottom B_3 triangle and one 7c-2e delocalized σ bond on the top B_4 pyramid and bottom B_3 triangle. (b) Four radial π CMOs for three delocalized π bonds on waist and one delocalized π bond on top B_4 pyramid and bottom B_3 triangle. (c) Three tangential π CMOs for three delocalized π bonds on waist.

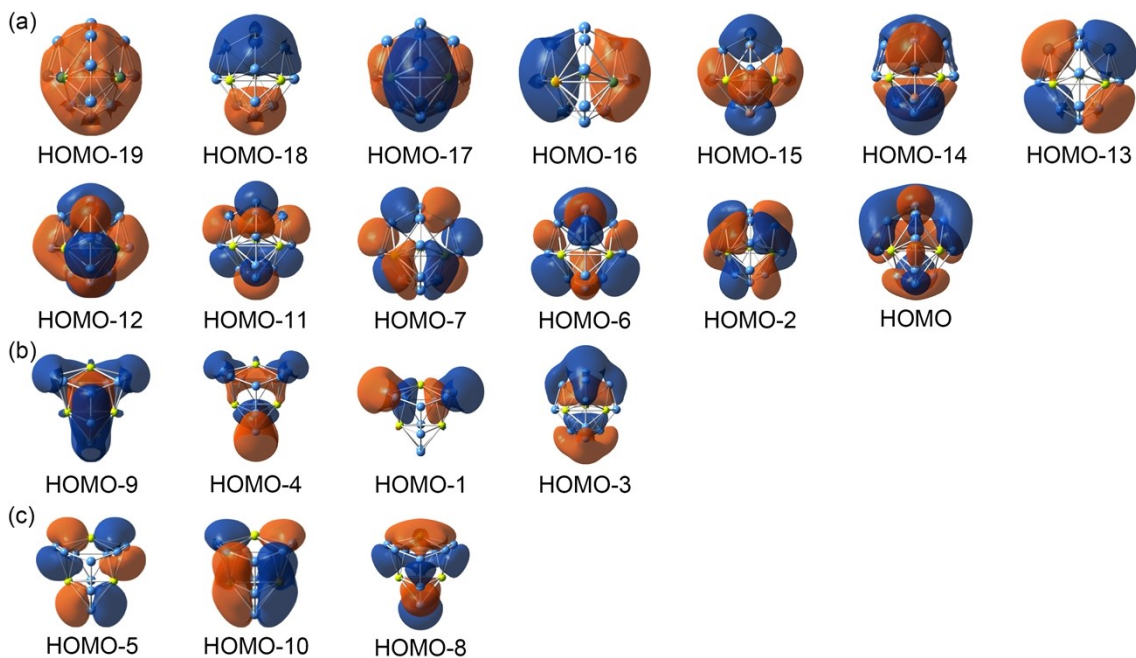


Figure S8. Electron localization functions (ELFs) for (a) the GM (C_{2v} , 1A_1), (b) the LM (C_s , $^1A'$) and (c) the TS (C_1 , 1A) structures.

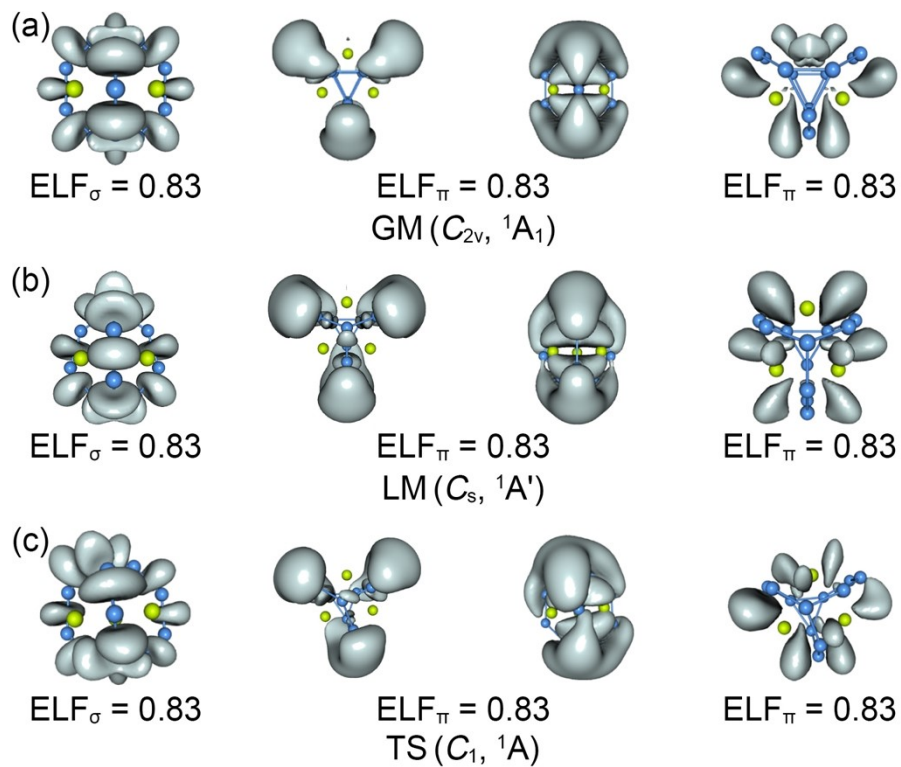


Figure S9. The CMOs for the TS (C_1 , 1A) of $\text{Be}_3\text{B}_{11}^-$ cluster. (a) Thirteen σ CMOs for eleven $2c-2e$ B–B σ bonds in B_{11} skeleton, one $3c-2e$ σ bonds on bottom B_3 triangle and one $7c-2e$ delocalized σ bond on top B_4 pyramid bottom B_3 triangle. (b) Four radial π CMOs for three delocalized π bonds on waist and one delocalized π bond on top B_4 pyramid and bottom B_3 triangle. (c) Three tangential π CMOs for three delocalized π bonds on waist.

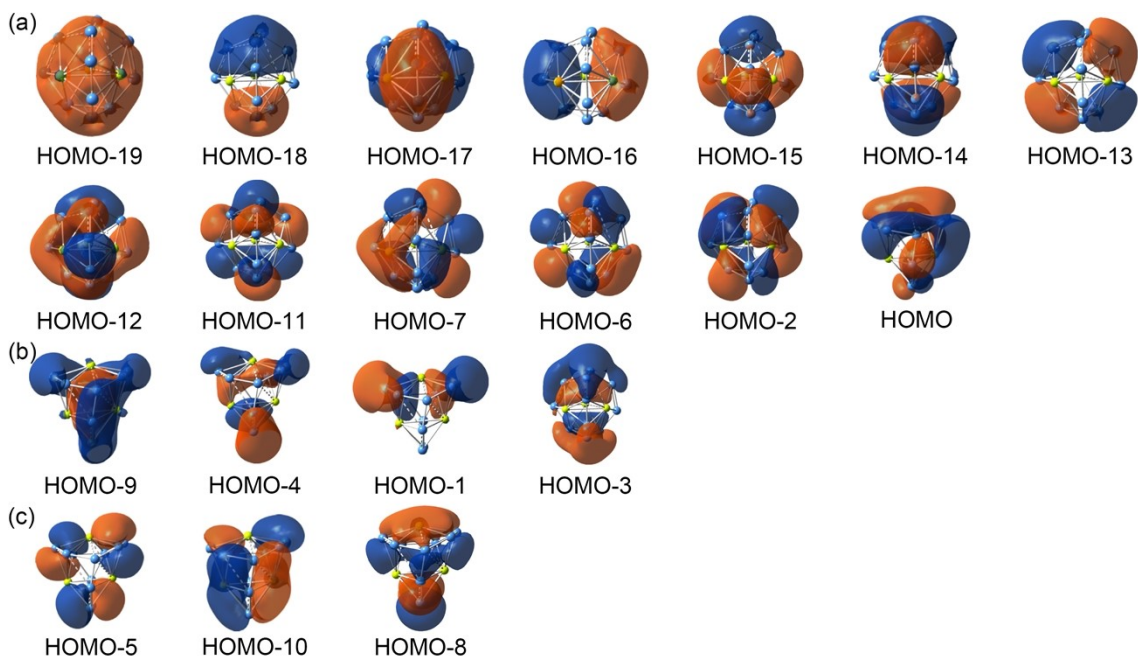


Figure S10. The adaptive natural density partitioning (AdNDP) bonding pattern for the TS (C_{1v} , 1A) structure of $\text{Be}_3\text{B}_{11}^-$ cluster. The occupation numbers (ONs) are indicated.

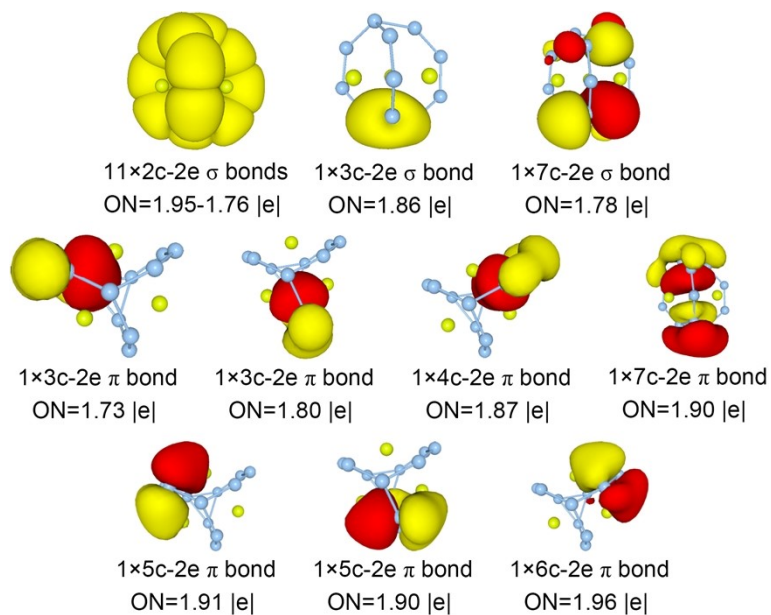


Figure S11. The evolution process of the delocalized (a) 6c-2e σ bond and (b) 6c-2e π bond on two B_3 triangles during the interconversion between the GM and LM.

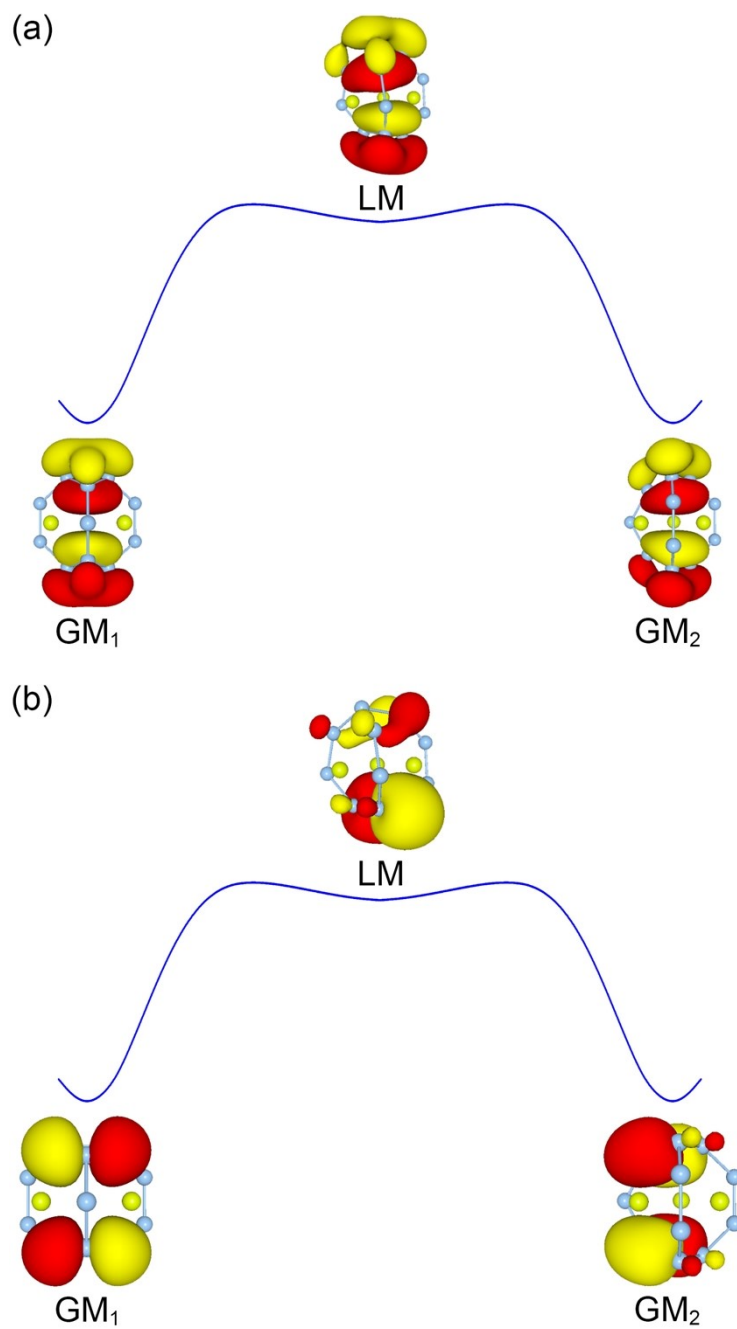


Table S1. Cartesian coordinates for (a) the global-minimum (GM) (C_{2v} , 1A_1), (b) the local minimum (LM) (C_s , $^1A'$), and (c) the transition state (TS) (C_1 , 1A) structures of $Be_3B_{11}^-$ cluster at the PBE0/6-311+G* level.

(a) GM (C_{2v} , 1A_1)

B	0.78814700	1.72234800	-0.28463500
B	1.89194400	0.76206000	-0.92078100
B	1.89194400	-0.76206000	-0.92078100
B	0.78814700	-1.72234800	-0.28463500
B	-0.78814700	-1.72234800	-0.28463500
B	-1.89194400	-0.76206000	-0.92078100
B	-1.89194400	0.76206000	-0.92078100
B	-0.78814700	1.72234800	-0.28463500
B	0.00000000	1.32009900	1.25416200
B	0.00000000	0.00000000	2.10125800
B	0.00000000	-1.32009900	1.25416200
Be	-1.33685700	0.00000000	0.74955200
Be	1.33685700	0.00000000	0.74955200
Be	0.00000000	0.00000000	-1.23399800

(b) LM (C_s , $^1A'$)

B	1.95382700	0.32161400	0.00000000
B	1.85257700	-1.22519100	0.00000000
B	0.67593300	-2.20138200	0.00000000
B	-0.81980800	-1.75839700	0.00000000
B	-1.54609900	-0.50410300	-0.84801500

B	-0.95895900	0.63557200	-1.80931200
B	0.24898400	1.49356700	-1.37890900
B	1.14715300	1.69340700	0.00000000
B	0.24898400	1.49356700	1.37890900
B	-0.95895900	0.63557200	1.80931200
B	-1.54609900	-0.50410300	0.84801500
Be	-1.10312800	1.11408900	0.00000000
Be	0.36560500	-0.60712100	1.17993400
Be	0.36560500	-0.60712100	-1.17993400

(c) TS (C₁, ¹A)

B	-0.04852900	1.95010800	-0.26736200
B	1.45504600	1.62124900	-0.48223900
B	2.21657700	0.29683200	-0.48325400
B	1.58716500	-1.09746500	-0.15207800
B	0.15737700	-1.78208300	-0.52902700
B	-1.09140900	-1.26589800	-1.40623200
B	-1.76025400	0.10104900	-1.20491400
B	-1.50323800	1.33664600	-0.15548300
B	-1.06154000	0.84696900	1.38679200
B	-0.39740000	-0.39050900	2.04179100
B	0.42759900	-1.37271000	1.10522200
Be	-1.24351000	-0.86014500	0.42079500
Be	0.93671500	0.48264200	1.00399400
Be	0.33005300	0.07226600	-1.24130900